Medicine®

CLINICAL CASE REPORT

OPEN

Computer Tomography Imaging Findings of Abdominal Follicular Dendritic Cell Sarcoma

A Report of 5 Cases

Jing Li, MD, Zhi-Jun Geng, MD, Chuan-Miao Xie, MD, PhD, Xin-Ke Zhang, MD, Rui-Ying Chen, MD, Pei-Qiang Cai, MD, PhD, and Xiao-Fei Lv, MD, PhD

Abstract: Follicular dendritic cell sarcoma (FDCS) is a neoplasm that arises from follicular dendritic cells. FDCSs originating in the abdomen are extremely rare. Clinically, they often mimic a wide variety of other abdominal tumors, and correct preoperative diagnosis is often a challenging task. To date, only scattered cases of abdominal FDCS have been reported and few data are available on their radiological features. Here we present the computer tomography imaging findings of 5 patients with surgically and pathologically demonstrated abdominal FDCS.

An abdominal FDCS should be included in the differential diagnosis when single or multiple masses with relatively large size, well- or ill-defined borders, complex internal architecture with marked internal necrosis and/or focal calcification, and heterogeneous enhancement with ''rapid wash-in and slow wash-out'' or ''progressive enhancement'' enhancement patterns in the solid component are seen.

(*Medicine* 95(1):e2404)

Abbreviations: CT = computed tomography, FDCS = follicular dendritic cell sarcoma.

INTRODUCTION

Follicular dendritic cells are nonlymphoid, nonphagocytic, antigen-presenting cells of the immune system.[1] Their main functions are to capture, process, and present antigens and immune complexes to B- and T-cells.[1] Follicular dendritic cell sarcoma (FDCS) is a neoplasm that arises from these follicular dendritic cells, and this rare primary neoplasm was first recognized in 1986 by Monda et al[2]; since then, approximately 200 cases of FDCS have been reported in the English language literature.[3] The majority of cases have been observed in the lymph nodes, particularly in the cervical lymph nodes and occasionally in the axillary and mediastinal lymph nodes. Approximately one-third of the reported cases have been located in an extranodal site.[4] The abdominal region is thought to be one of the relative preferred sites of extranodal FDCS.[4] Clinically, they often mimic a wide variety of other abdominal tumors, and correct preoperative diagnosis is often a challenging task.

To date, only scattered cases of abdominal FDCS have been reported in the English literature, most of which were case reports[5,6]; these reports have mainly focused on pathological and clinical features.[4] To the best of our knowledge, there have been only a few studies describing the imaging features of abdominal FDCS.[7–10] We therefore retrospectively reviewed the computed tomography (CT) findings of 5 patients with surgically and pathologically demonstrated abdominal FDCS.

MATERIALS AND METHODS

Patient Data

The study protocol was approved by the Institutional Review Board of Sun Yat-sen University Cancer Center. Five cases of FDCS confirmed by surgery and pathology were collected from our 2 hospitals from January 2006 to July 2015. All 5 patients had undergone a complete or partial surgical resection of their tumor, and the resection specimens were collected and analyzed at 2 central pathology laboratories. The definitive diagnosis of FDCS was established by histological and immunohistochemical evaluations. The medical records, including a history of the disease, radiologic imaging, and pathological data for all 5 patients, were retrieved for retrospective analysis.

Equipment and Methods

CT examinations were performed at 4 spiral CT scanners (Aquilion 16, Toshiba Medical system, Otawara, Japan, n = 2; Brilliance iCT256, Philips Medical Systems, Best, The Netherlands, n = 1; LightSpeed 16, GE Health Care, Milwaukee, WI, n = 1; Dual Source CT, Somatom Definition, Siemens Medical Systems, Forchheim, Germany; n = 1). All 5 patients underwent noncontrast- and contrast-enhanced CT scans. The scan parameters were as follows: 2 to 5 mm slice thickness reconstructions, 23 cm field of view, 120 kV voltage, 200 to 300 mA current, and 256 × 256 matrix. An intravenous bolus dose of 80 to 100 mL of a nonionic iodine contrast agent (iopromide;

Editor: Patrick Wall.
Received: August 11, 2015; revised: December 5, 2015; accepted: December 9, 2015.
From the Department of Medical Imaging (JL, Z-JG, C-MX, P-QC, X-FL), Collaborative Innovation Center for Cancer Medicine, State Key Laboratory of Oncology in South China, Sun Yat-sen University Cancer Center; Department of Pathology (X-KZ), Sun Yat-sen University Cancer Center; and Department of Medical Imaging Center (R-YC), NanFang Hospital, Southern Medical University, Guangzhou, PR China.
Correspondence: Xiao-Fei Lv and Pei-Qiang Cai, Department of Medical Imaging, Collaborative Innovation Center for Cancer Medicine, State Key Laboratory of Oncology in South China, Sun Yat-sen University Cancer Center, 651 Dongfeng East Road, Guangzhou 510060, PR China (e-mail: lvxiaofei_1984@163.com; caipq_image@163.com).
JL and Z-JG contributed equally to this work as co-first authors.
This work was supported by the Natural Science Foundation of China (Grant No. 81401399), Medical Scientific Research Foundation of Guangdong Province (Grant No. B2014162), and the Fundamental Research Funds for the Central Universities (15ykpy35). The funders had no role in study design, data collection and analysis, decision to publish, or preparation of the manuscript.
The authors have no conflicts of interest to disclose.

ISSN: 0025-7974
DOI: 10.1097/MD.0000000000002404

Ultravist; Schering) was injected into the antecubital vein at a rate of 2.5 to 3.0 mL/s to the patients who underwent contrast-enhanced CT. Multiphase enhancement images, including arterial, venous, and delayed-phase studies, were obtained at 25 to 35, 60 to 70, and 180 to 300 seconds after the initiation of intravenous contrast agent injections.

Image Analysis

Two experienced abdominal radiologists retrospectively reviewed all the CT images in consensus. The CT imaging characteristics were analyzed with particular attention to the lesion location, shape, size, number, margins, attenuation in the unenhanced and enhanced CT images, enhancement patterns of the tumor, and the tumor-spread patterns (including local invasion, lymph node, and distant metastasis). The attenuation on unenhanced CT images was classified as low, moderate, or high with relative to the adjacent tissues. The degree of enhancement was evaluated objectively by the change in the CT values and categorized as none, mild, moderate, or marked. In addition, the presence of any calcification or necrosis within the lesion was also recorded.

RESULTS

Clinical Information

The study group included 4 males and 1 female, with a mean age of 60 years (range, 55–70 years). Two patients were asymptomatic and were found incidentally. Two had complained of recurrent or persisting and increasing abdominal discomfort, which included abdominal pain and abdominal fullness, with symptom durations of 1 month and 5 years, respectively. The remaining patient complained of right upper abdominal pain with 1 month's duration combined with fever for 6 days. Routine laboratory tests revealed that the patient who had a fever showed elevated white cell counts. The results of routine laboratory tests for the remaining 4 patients revealed no significant abnormalities. Serum tumor marker examinations, including CEA (n = 5), CA199 (n = 5), and CA724 (n = 3), were performed, and none of these revealed any significant abnormalities in the 5 patients to whom they were administered.

CT Findings

The CT findings of all 5 patients are shown in Table 1. Two cases were single tumors (Figures 1 and 4) and 3 cases (Figures 2, 3 and 5) showed multiple tumors, with 8 tumors in total. All tumors were located within the intra-abdominal region and/or the retroperitoneum. The tumors ranged from 5.3 to 17.1 cm (average 9.6 cm) in the largest diameter. All tumors were ovoid (n = 5), lobulated (n = 2), or irregular (n = 1), with well-defined (n = 5) or partially ill-defined margins (n = 3).

On unenhanced CT, 7 lesions presented as a heterogeneous soft-tissue mass with intratumoral patchy or irregular low-attenuating areas (n = 6, Figures 1A, 2A, 3A, and 4A) and/or scattered coarse and/or chunk-like calcifications (n = 4, Figures 1A, 3A, and 5A). The remaining one showed relatively homogeneous density (Figure 5E). The average CT density of the solid component in all lesions was 40.1 HU (range, 31–47 HU). During contrast-enhanced multiphase scans, all 8 tumors showed heterogeneous enhancement with their solid parts demonstrating marked (n = 4, Figures 1B–E, 2F, and 3B–F) or moderate (n = 4, Figures 2A–E, 4B–D, and 5) enhancement. The density values of the solid components in the 6 masses (Figures 1B–D, 2B–D, 3B–D, and 4B–D) were 56 to 152 HU (average, 93.1 HU), 65 to 112 HU (average, 92.5 HU), and 60 to 126 HU (average, 89.0 HU) on arterial, venous, and delayed phase images, respectively, with a ''rapid wash-in and slow wash-out'' pattern of enhancement. The density values of the solid components in the remaining 2 masses (case 5, Figure 5) were 56 to 64 HU (average, 62.0 HU), 64 to 72 HU (average, 68.0 HU), and 67 to 78 HU (average, 73.0 HU) on 3 enhanced phase images, respectively, with a ''progressive enhancement'' pattern of enhancement. Intratumoral serpentine feeding arteries or peritumoral draining veins were observed in 2 lesions (Figures 1B and 2B). Six lesions presented with patchy or irregular nonenhanced areas during enhanced phases, which suggests necrotic components.

Local invasion was noted in 3 tumors. Tumor 2 (Figure 2A–E) surrounded and encased the left kidney, the renal artery, and the vein of the left renal hilum, with widespread involvement of the adjacent perirenal fascia and peritoneum. It was accompanied by renal vein and inferior vena cava thrombus. Tumors 3 (Figure 2F) and 4 (Figure 3A–E) involved the left psoas muscle and duodenal bulb, respectively. Peritumoral lymph nodes were noted in 6 tumors (Figures 1E, 2E, F, and 3E), with the shorter diameters ranging from 0.5 to 2.1 cm and some of them demonstrating marked internal necrosis (Figure 1E). Two patients had distant metastasis in the liver at the time of diagnosis (Figure 1F).

Pathological Findings

Six tumors in 4 cases were completely surgically resected. Two tumors in 1 patient (case 2) had extensive infiltration and only underwent excision biopsy. Macroscopically, the 6 complete resected lesions were oval or irregular, with a complete or partial capsule. Microscopically, the tumor was composed of proliferations of spindled to ovoid cells, with a variety of growth patterns including whorled, storiform, fascicular, and nodular, associated with lymphocyte-rich stromas (Figure 1H). Giant cells and mitotic figures were identified occasionally. Irregular hemorrhage and/or coagulative necrosis were observed in all cases. Immunohistochemical examination revealed that the tumors were positive for CD21 (4/4), CD35 (4/4), CD23 (4/4), CD68 (2/4), Vimentin (4/4), BCL-2 (3/3), S-100 (1/5), EMA (1/5), and CD34 (1/5) in each instance where they were applied.

Follow-Up

Two of 5 patients underwent chemotherapy followed by surgery. One of them (case 4) went into remission during the 11-month follow-up period after the surgery. Another patient (case 1) had metastases develop in the liver 4 months later (Figure 1G). For the remaining 3 patients, 1 patient (case 3) who underwent surgery without chemotherapy remained disease-free for 2 months. The other 2 were lost to follow-up.

DISCUSSION

Extranodal FDCS was first reported by Chan et al in 1994.[11] Since then, the spectrum of FDCS in extranodal sites has greatly expanded to include locations throughout the body.[4] The more predominant extranodal sites for tumor involvement include the tonsils, pharyngeal region, thyroid, mediastinum, intra-abdominal, and the retroperitoneum.[4,12] Histologically, the most commonly identified feature of this entity is the presence of oval to spindle cells with elongated nuclei, delicate, dispersed chromatin, and pale eosinophilic cytoplasm.[13] Immunohistochemically, FDCS cells generally share the

TABLE 1. Computed Tomography Findings of 5 Cases of Follicular Dendritic Cells

Case No./Age, y/Sex	Tumor No.	Tumor Location	Size (cm × cm)	Gross Morphology (Shape/Margin)	Unenhancement (Density/Calcification/Necrosis)	Enhancement (Degree/Pattern)	Tumor-Spread Patterns (Local Invasion/Lymph Node/Distant Metastases)
1/57/F	1	Mesentery	14.8 × 9.1	Oval/well-defined	Heterogeneous/yes/yes	Marked heterogeneous/ rapid wash-in and slow wash-out	None/peritumoral lymph node/liver metastases
2/70/M	2	Mesentery and retroperitoneum	17.1 × 13.2	Irregular/partially ill-defined	Heterogeneous/none/yes	Moderate/heterogeneous/ rapid wash-in and slow wash-out	Local invasion (tumors 2 and 3), renal vein and inferior vena cava thrombus (tumor 2)/ peritumoral lymph node (tumors 2 and 3)/liver metastases
	3	Retroperitoneum	6.5 × 6.4	Oval/partially ill-defined	Heterogeneous/none/yes	Marked/heterogeneous/ rapid wash-in and slow wash-out	
3/58/F	4	Abdominal cavity	5.6 × 4.8	Lobulated/partially ill-defined	Heterogeneous/yes/yes	Marked/heterogeneous/ rapid wash-in and slow wash-out	Local invasion (tumor 4)/ peritumoral lymph node (tumor 4)/none
	5	Greater omentum	5.3 × 3.9	Oval/well-defined	Heterogeneous/none/yes	Marked/heterogeneous/ rapid wash-in and slow wash-out	
4/55/F	6	Retroperitoneum	11.7 × 9.1	Oval/well-defined	Heterogeneous/none/yes	Moderate/heterogeneous/ rapid wash-in and slow wash-out	None/none/none
5/60/F	7	Mesentery	9.0 × 8.4	Lobulated/well-defined	Heterogeneous/yes/no	Moderate/heterogeneous/ progressive enhancement	None/peritumoral lymph node (tumors 7 and 8)/ none
	8	Retroperitoneum	6.7 × 5.2	Oval/well-defined	Homogeneous/yes/no	Moderate/heterogeneous/ progressive enhancement	

F = female, M = male.

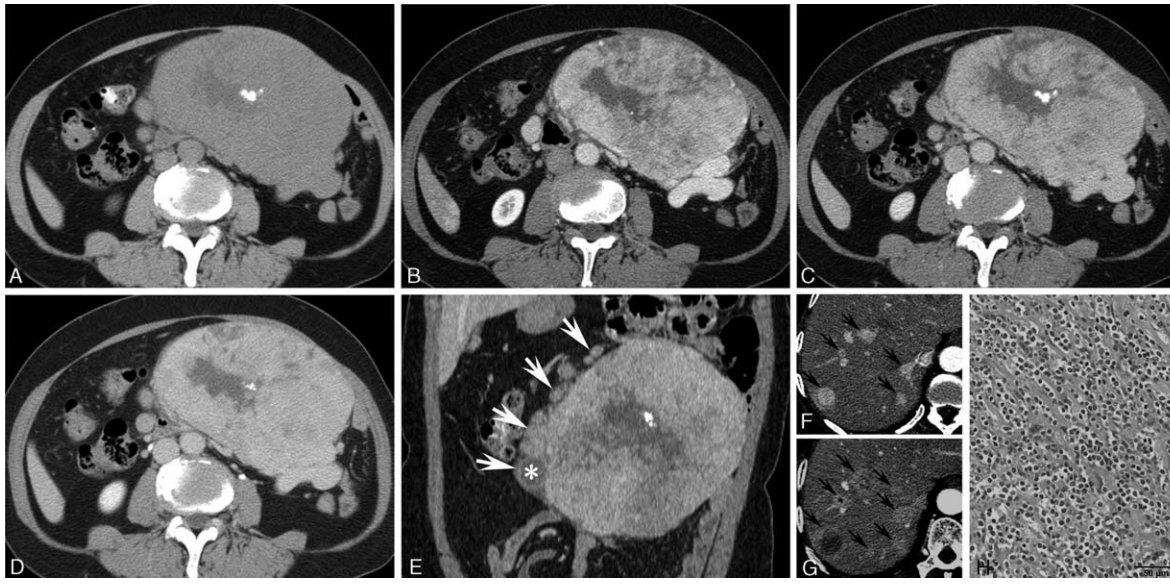

FIGURE 1. Case 1. FDCS arising from the mesentery in a 57-year-old woman. (A) The unenhanced CT imaging showed a large, well-defined heterogeneous mass (tumor 1) with patchy low-attenuating necrotic areas and coarse calcifications located centrally. (B–D) The enhanced multiphase CT images revealed marked heterogeneous enhancement with a ''rapid wash-in and slow wash-out'' pattern of enhancement in the solid component, accompanied by peritumoral serpentine draining veins. (E) Coronal reconstruction disclosed that there were multiple peritumoral lymph nodes (arrow), with some showing marked internal necrosis (white star). (F) Enhanced CT image showed multiple nodules in the right liver lobe with marked enhancement on arterial phase images (black arrow), which revealed distant metastasis. (G) After 4 months of follow-up, enhanced CT image showed the progression of hepatic metastasis. (H) The tumor was composed of spindle cells that were arranged in a fascicular pattern, and the spindle cells were admixed with lymphocytes (hematoxylin & eosin stain, ×200).

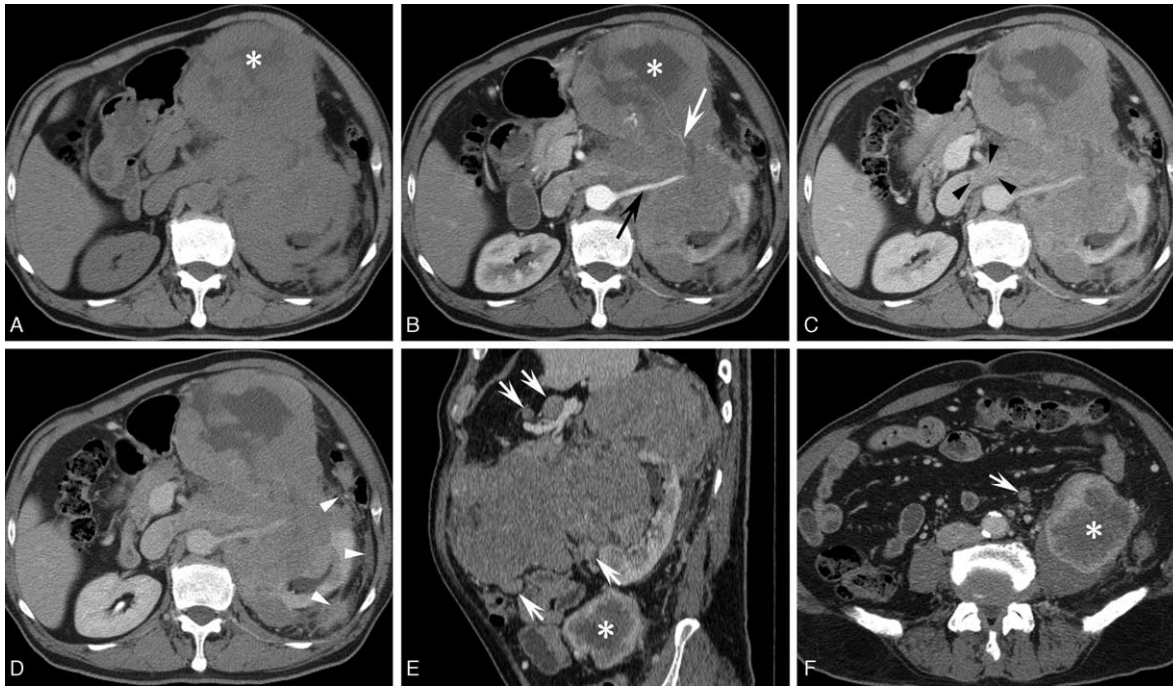

FIGURE 2. Case 2. FDCS with wide involvement of the mesentery and retroperitoneum in a 70-year-old man. (A) Unenhanced CT imaging showed a large, irregular, partially ill-defined mass (tumor 2) with intratumoral irregular necrosis (white star). (B–D) The enhanced multiphase CT images revealed a moderately heterogeneous tumor with a ''rapid wash-in and slow wash-out'' pattern of enhancement in the solid component, with serpentine vessels (white arrow) on arterial phase images, with the renal vessels of the left renal hilum encased (black arrow), widespread adjacent perirenal fascia and peritoneum involvement (white arrowheads), accompanied by renal vein and inferior vena cava thrombus (black arrowheads). (E) The sagittal reconstruction enhanced image also showed multiple peritumoral lymph nodes (short white arrows). Another mass (tumor 3) with marked internal necrosis located at the left retroperitoneum was also observed. (F) Lower abdominal enhanced CT image showed another oval, partially ill-defined mass (tumor 3) located at the left retroperitoneum with marked heterogeneous enhancement, marked internal necrosis (white star), and peritumoral lymph nodes (short white arrows).

FIGURE 3. Case 3. FDCS located in the right upper abdominal cavity in a 58-year-old woman. (A) The unenhanced CT imaging showed a partially ill-defined heterogeneous mass (tumor 4) located in patchy, low-attenuating areas with coarse and chunk-like calcifications. (B–D) The enhanced multiphase CT images revealed marked heterogeneous enhancement with a ''rapid wash-in and slow wash-out'' pattern of enhancement and internal necrosis (white star). (E) Coronal reconstruction found that the tumor was located near the duodenal bulb and shared an unclear boundary with it (white arrow). Peritumoral lymph node was observed (white arrowhead). (F) Enhanced CT image showed another oval, well-defined mass (tumor 5) located at the greater omentum with marked heterogeneous enhancement and internal necrosis (white star).

immunophenotype of non-neoplastic FDCs, and positive staining of CD21, CD35, and CD23 was particularly useful for the final diagnosis of FDC.[3,13]

Extranodal FDCS can present between 9 and 82 years of age (mean age, 46 years) and has a slight female predominance (female-to-male ratio, 77:65).[12] FDCSs originating in the abdomen are rare.[12] Because of their scarceness and the limited number of reports, the exact incidence of these entities is still unknown. In the current case series of abdominal FDCS, the ages of the patients were in the range of 55 to 70 years (mean age, 60 years), and there was an obvious predilection for females, with a female-to-male ratio of 4:1. Clinically, most patients were asymptomatic or presented with abdominal fullness, abdominal pain, or symptoms related to the compression of adjacent structures.[5–8,10,14] The serum tumor marker examinations (including CEA, CA199, and CA724) performed in the present study showed no specificity.

Various sites of FDCS originating from the abdomen have been reported, including the liver,[12] spleen,[3] pancreas,[15] adrenal gland,[3] gastrointestinal tract,[10,12] retroperitoneum,[5] mesentery,[8] omentum,[7] and abdominal wall.[16] Abdominal FDCS has been reported to tend to manifest larger-sized tumors than those outside the abdomen and exhibited an average tumor size of 10.2 cm (range, 3–22 cm).[12] Our findings were in accordance with these observation.

CT imaging features aid in making correct diagnoses before treatment when a neoplasm is detected. In the few published reports,[7–10] abdominal FDCS has been described as a discrete mass with complex internal architecture, such as heterogeneous enhancement, marked by internal necrosis and focal calcification. In our cases, most lesions showed well- or partially ill-defined heterogeneous density tumors with soft-tissue parts and patchy or irregular low-attenuating areas. The soft-tissue parts corresponded histologically to the tumor's solid portion, and demonstrated heterogeneous enhancement on postcontrast CT scans. The low-attenuating areas that were correlated with necrosis and hemorrhage showed no enhancement. Frequent necrosis and/or hemorrhage observed in abdominal FDCS are thought to be related to the relatively large size of these tumors. Calcifications can be detected on unenhanced CTs in quite a few cases, and the pattern of calcifications has always been depicted as coarse and/or chunk-like in previous studies.[7,10] In our series, 50% (4/8) of all tumors also showed scattered coarse and/or chunk-like calcifications located centrally or eccentrically. These imaging findings described above are similar to those in previous reports and demonstrate that the internal necrosis and coarse and/or chunk-like descriptions may be relatively characteristic CT imaging features for diagnosing abdominal FDCS.

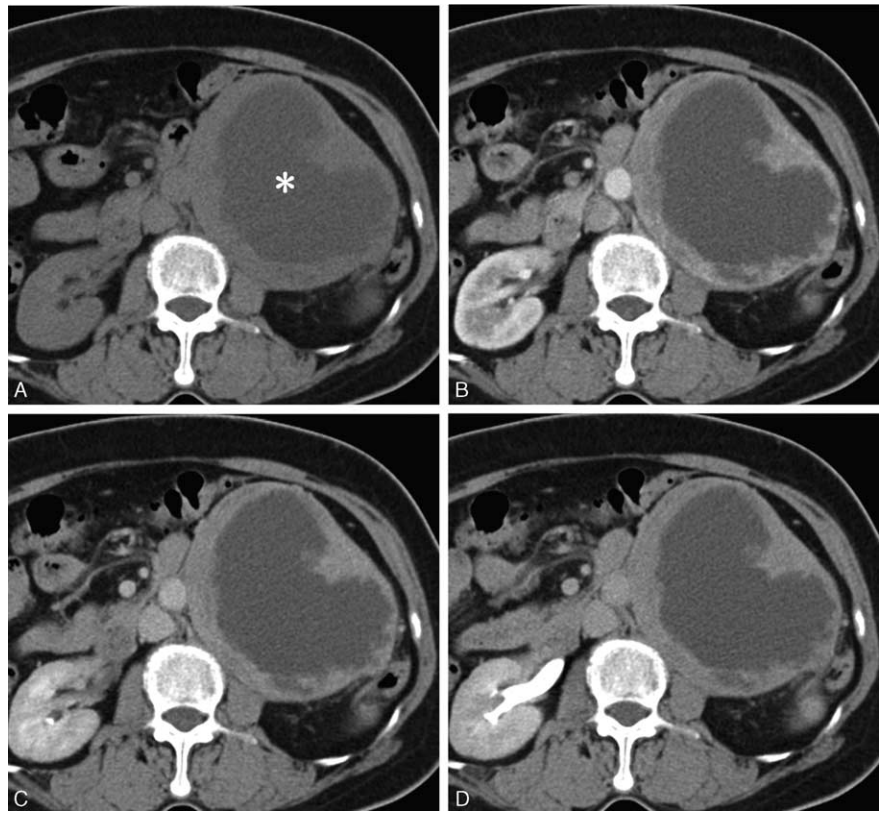

FIGURE 4. Case 4. FDCS arising from the left retroperitoneum in a 55-year-old woman. (A) The unenhanced CT imaging showed a large, well-defined heterogeneous mass with patchy low-attenuating areas located centrally (white star). (B–D) The enhanced multiphase CT images revealed moderate heterogeneous enhancement with a ''rapid wash-in and slow wash-out'' pattern of enhancement in the solid component and internal necrosis located centrally.

FIGURE 5. Case 5. FDCS arising from the mesentery in a 60-year-old woman. (A) The unenhanced CT imaging showed a lobulated, well-defined heterogeneous mass (tumor 7) with intratumoral coarse and chunk-like calcifications. (B–D) The enhanced multiphase CT images revealed moderate heterogeneous enhancement. The average density values of the solid component in the region of interest revealed a ''progressive enhancement'' pattern. (E–H) Middle abdominal CT image showed another oval, well-defined mass (tumor 8) located at the retroperitoneum with moderate heterogeneous enhancement. The average density values of the solid component in the region of interest revealed a ''progressive enhancement'' pattern.

To our knowledge, the enhancement patterns in multiphase CT imaging findings of abdominal FDCS have not been previously reported.[7–10] In the present series, the solid component of the tumors showed marked or moderate enhancement with ''rapid wash-in and slow wash-out'' or ''progressive enhancement'' patterns of enhancement during multiphase imaging. The finding of marked or moderate enhancement of all tumors in the present study is consistent with some previous studies.[7–10] In addition, serpentine feeding arteries and draining veins in and/or around the tumor were noted in 2 lesions. These findings suggest that abdominal FDCS may be relatively hypervascular, or at least not hypovascular, as has been reported previously in some mediastinal FDCSs.[17] The patterns of ''slow wash-out'' and ''progressive enhancement'' in the venous and delayed phases are thought to correlate with hypercellular density areas with proliferation of spindled to ovoid cells and to be associated with lymphocyte-rich stromas.

Extranodal FDCSs are more aggressive than a low-grade soft tissue sarcoma, and they should at minimum be considered as an intermediate-grade malignancy.[4,12,18] They often metastasize via the blood and the lymphatic system.[4] Lymph nodes, lung, and liver are the most common sites for metastasis.[3] Surgical resection for localized disease remains the mainstay of treatment, and the possible roles for adjuvant radiotherapy and chemotherapy remain undefined.[4,12] The overall recurrence, metastasis, and mortality rates of extranodal FDCS cases were 49.2%, 21.5%, and 13.8%, respectively.[12]

Differential diagnosis of FDCS in the abdomen region should include abdominal mesenchymal neoplasms such as leiomyosarcoma, malignant fibrous histiocytoma, fibrosarcoma, gastrointestinal/extragastrointestinal stromal tumor and solitary fibrous tumor, and neurogenic tumors. Similarities on clinical imaging between the above tumors and FDCS are noted. Given the rarity of abdominal FDCS, prospective imaging diagnosis of this type of tumor can be challenging; all final diagnoses depend upon histopathological testing.

In conclusion, abdominal FDCSs arising from the abdomen are rare, occurring predominantly in the middle-aged and elderly. During CT imaging, the possibility of FDCS should be considered when single or multiple masses originate from the intra-abdominal region and/or the retroperitoneum, with relatively larger sizes, complex internal architectures with marked internal necrosis and/or focal coarse and/or chunk-like calcifications, and heterogeneous enhancement with ''rapid wash-in and slow wash-out'' or ''progressive enhancement'' patterns of enhancement in the solid component. Regional lymphadenopathy is always noted.

REFERENCES

1. Tew JG, Kosco MH, Burton GF, et al. Follicular dendritic cells as accessory cells. *Immunol Rev.* 1990;117:185–211.
2. Monda L, Warnke R, Rosai J. A primary lymph node malignancy with features suggestive of dendritic reticulum cell differentiation. A report of 4 cases. *Am J Pathol.* 1986;122:562–572.
3. Wang H, Su Z, Hu Z, et al. Follicular dendritic cell sarcoma: a report of six cases and a review of the Chinese literature. *Diagn Pathol.* 2010;5:67.
4. Li L, Shi YH, Guo ZJ, et al. Clinicopathological features and prognosis assessment of extranodal follicular dendritic cell sarcoma. *World J Gastroenterol.* 2010;16:2504–2519.
5. Yuan T, Yang Q, Zhang H, et al. A 46-year-old Chinese woman presenting with retroperitoneal follicular dendritic cell sarcoma: a case report. *J Med Case Rep.* 2014;8:113.
6. Shaw D, Cuison R, Ito H. Follicular dendritic cell sarcoma of the stomach: case report and review of the literature. *Curr Oncol.* 2014;21:775–778.
7. Chien JC, Lao WT, Chen C, et al. Follicular dendritic cell sarcoma of the omentum: multidetector computed tomography findings. *Korean J Radiol.* 2013;14:213–217.
8. Li Z, Jin K, Yu X, et al. Extranodal follicular dendritic cell sarcoma in mesentery: a case report. *Oncol Lett.* 2011;2:649–652.
9. Long-Hua Q, Qin X, Ya-Jia G, et al. Imaging findings of follicular dendritic cell sarcoma: report of four cases. *Korean J Radiol.* 2011;12:122–128.
10. Kang TW, Lee SJ, Song HJ. Follicular dendritic cell sarcoma of the abdomen: the imaging findings. *Korean J Radiol.* 2010;11:239–243.
11. Chan JK, Tsang WY, Ng CS. Follicular dendritic cell tumor and vascular neoplasm complicating hyaline-vascular Castleman's disease. *Am J Surg Pathol.* 1994;18:517–525.
12. Wang RF, Han W, Qi L, et al. Extranodal follicular dendritic cell sarcoma: a clinicopathological report of four cases and a literature review. *Oncol Lett.* 2014;9:391–398.
13. Soriano AO, Thompson MA, Admirand JH, et al. Follicular dendritic cell sarcoma: a report of 14 cases and a review of the literature. *Am J Hematol.* 2007;82:725–728.
14. Diaz DLA, Garde C, Artieda C, et al. Intra-abdominal follicular dendritic cell sarcoma. *Clin Transl Oncol.* 2006;8:837–838.
15. Shen SC, Wu CC, Ng KF, et al. Follicular dendritic cell sarcoma mimicking giant cell carcinoma of the pancreas. *Pathol Int.* 2006;56:466–470.
16. Schwarz RE, Chu P, Arber DA. Extranodal follicular dendritic cell tumor of the abdominal wall. *J Clin Oncol.* 1999;17:2290–2292.
17. Leipsic JA, Mcadams HP, Sporn TA. Follicular dendritic cell sarcoma of the mediastinum. *Am J Roentgenol.* 2007;188:W554–W556.
18. Chan JK, Fletcher CD, Nayler SJ, et al. Follicular dendritic cell sarcoma. Clinicopathologic analysis of 17 cases suggesting a malignant potential higher than currently recognized. *Cancer.* 1997;79:294–313.